27th ABCM International Congress of Mechanical Engineering
December 04-08, 2023, Florianópolis-SC, Brazil

# COB-2023-0736
# WEAR RESISTANCE EVALUATION OF THE COATING DIN 8555: MF 10-GF-60-GRZ ON THE HARDOX® 450 STEEL APPLIED IN THE RECOVERY OF MINING TRUCK BODY

**Thais Stefany Santiago Brandão**
**Gilmar Cordeiro da Silva**
PUC Minas – Graduate Program in Mechanical Engineering, Av. Dom José Gaspar, 500, 30.535-901, Belo Horizonte – MG, Brazil.
thaisfany1@hotmail.com
gilmarcord@gmail.com

**Anderson Junior dos Santos**
UFMG – Universidade Federal de Minas Gerais, Av. Pres. Antônio Carlos, 6627, 31.270-901, Belo Horizonte – MG, Brazil.
andersonsantos@cefetmg.br

***Abstract.*** *In the mining industry, equipment deterioration due to abrasive wear can lead to reduced future revenue and to increase equipment availability, abrasion resistant plates and coatings are used. Hardox® steel is used in the manufacture of off-road truck tippers. In this sense, this work proposed a study for the application of the hard coating DIN 8555: MF 10-GF-60-GRZ, in the areas of greater incidence of wear on the body, as an alternative to protect the base metal in search of increased durability and, consequently, the extension of the working hours of the equipment. The present study aimed to evaluate whether the material could be used for coating Hardox® 450 by the flux-cored welding process (FCAW), to compare the performance of coated and uncoated sheets about abrasive wear. The methodology consisted of the evaluation of metallic properties, with chemical analysis, traction test and comparison of wear resistance through the pin-on-disk test. With the results obtained, it was possible to verify that the properties of the hard coating were compatible with the base metal, therefore with its application it is possible to have good efficiency in the operation.*

***Keywords:*** *Wear, Hardox® 450, Hardfacing, Welding, Pin-on-disk*

## 1. INTRODUCTION

In the contemporaneity of the 21st century, the world is constantly changing in all spheres of organizations, making the development of devices and equipment increasingly complex. This makes a thorough management analysis necessary, with the need to define goals and priorities so that the equipment becomes more efficient and competitive. According to Oliveira (2020), the satisfactory availability of equipment suggests the production capacity of an organization and, consequently, the reduction of costs and the guarantee of good product quality.

As reported by IBRAM (Brazilian Institute of Mining) in 2021, the mineral sector recorded a 62% increase in revenue compared to 2020, totaling R$ 339.1 billion (excluding oil and gas) and Brazilian mineral exports reached US $58 billion, an increase of 58.6% compared to 2020. Through various industrial processes with state-of-the-art technology, the ore is processed to later be sold to the steel industry.

During the extraction of the ore, the equipment used in the process deteriorates through abrasive wear of the area in contact with the mineral, due to the forces of impact and friction. The wear and tear of components and equipment in mining, as well as in other branches of activity, results in a reduction in future revenue, as it is an agent of capital depreciation, maintenance expenses, replacement of components and even the interruption of operations due to maintenance stops. When it comes to abrasive wear, the market and industry use plates and hardfacing with abrasion resistance to increase the availability of operation of mining equipment.

Highly abrasion resistant steels used in sheets and coatings have few alloying elements in low percentages in their chemical composition, with equivalent carbon in the order of 0.48 to 0.73, such as the Hardox® steels produced by Svenskt Stål Aktiebolag (SSAB) (ÖZTURAN *et al* , 2022). Generally, off-road truck buckets are manufactured in high hardness steels, such as highly manganese alloyed steels, high chromium cast iron and quenched and tempered low alloy steels, where these materials ensure good performance in wear conditions.

Hardfacing weld metal overlay refers to weld deposits made, using a variety of processes, to prevent the effects of wear and/or abrasion. This deposition can be carried out using different techniques, depending on the type of wear and thickness of the applied hardfacing layer. In general, it is performed using techniques associated with soldering processes, as it is versatile and has a range of possible alloys. The process has the advantage of being able to be applied in localized areas of the part that are more subject to wear, which can extend the useful life of the plates, both new and already worn. (INAVOV *et al* , 2022).

According to Costa, Vendramini and Ribeiro (2019), welding with tubular wire is a process in which the coalescence of metals is obtained through heating by an arc between a continuous tubular electrode (it performs the functions of stabilizing the arc and adjusting weld composition) and the part. This type of welding has two main variations:

a) Self-protected welding: consists of the internal flux that provides all the necessary protection in the arc region;

b) Gas Shield Welding: Shielding is provided by gas, similar to the GMAW process.

In both forms, the process is usually operated semi-automatically, using the same equipment as the GMAW process.

For the development of this work, Hardox® 450 steel will be chosen, manufactured by SSAB, by hot rolling and subjected to tempering heat treatment (LIGIER *et al.* , 2022). It has a nominal hardness of 450 HBW and is supplied in thicknesses from 3.2 to 130 mm (SSAB, 2021). And for the hardfacing, Ø 1.6 mm tubular wire will be chosen, which meets the classification AWS DIN 8555/MF-10-GF-60-GR provided by ESAB. In short, wear resistance is obtained by increasing hardness, so when a bucket undergoes maintenance, all wear plates are replaced, regardless of their condition.

In this sense, this dissertation proposes a study for the application of a hardfacing, in the areas with the highest incidence of wear, in an off-road truck. This additional layer of material can be an alternative to protect the base metal and recover the consumed parts in search of increased durability and, consequently, the extension of the working hours of the equipment, to avoid a stop for the total exchange of the plates.

## 2. EXPERIMENTAL DETAILS

In this study, Hardox® 450 steel was used as the base metal, supplied in the form of a thick plate with a thickness of 12.7 mm, and for the hardfacing, tubular wire of Ø 1.6 mm, which complies with the classification AWS DIN 8555/ MF-10-GF-60-G is a high-carbon, high-chromium cored wire with no added carbide formers, abrasion resistant, and stainless steel. For the deposition of this filler metal, the FCAW method was applied because it is a self-protected tubular wire.

The chemical compositions of Hardox® 450 and weld metal are given in Table 1 and the mechanical properties of the materials are given in Table 2 based on suppliers' certificates.

Table 1. Chemical composition of Hardox® 450 and deposited weld metal (%).

| **Material** | **C** | **Si** | **Mn** | **P** | **S** | **Cr** | **Ni** | **Mo** | **B** |
|---|---|---|---|---|---|---|---|---|---|
| Hardox® 450 (1) | 0.26 | 0.70 | 1.60 | 0.025 | 0.01 | 1.40 | 1.50 | 0.60 | 0.005 |
| Weld metal (2) | 4.00 | 0.77 | 0.082 | 0.006 | 0.026 | 21.74 | - | - | - |

(1) maximum values in (%)
(2) values found in the chemical analysis of the metal deposited in (%)

Table 2. Properties of Hardox® 450 and deposited weld metal.

| **Material** | Hardox® 450 | Weld metal |
|---|---|---|
| Tensile strength (MPa) | 1412 | 590 |
| Yield strength (MPa) | 1250 | 550 |
| Charpy-V (J) impact test | 50 | 65 |
| Temperature (°C) | -40 | -30 |
| Hardness (HRC) | 44.5 | 60 |

The welding of the plate for making the test specimens was performed using the FCAW process with a Deltaweld 852 model welding machine from Miller, where the voltmeter and ammeter were calibrated to ensure the reliability of the welding patterns.

The welding process was carried out with the parameters indicated in Table 3 and two layers of deposited material were applied over the entire surface. Shielding gas was not used, as the tubular wire is self-protected. In Figure 1 it is possible to observe the coated sheet.

Table 3. Welding parameters.

| **Welding process** | **FCAW** |
|---|---|
| Welding voltage (V) | 24.2 to 25.4 V |
| Welding current (A) | 183 to 195 A |
| Welding speed | 160 to 165 mm/min |
| Welding wire | DIN 8555 MF-10-GF-60-GR |

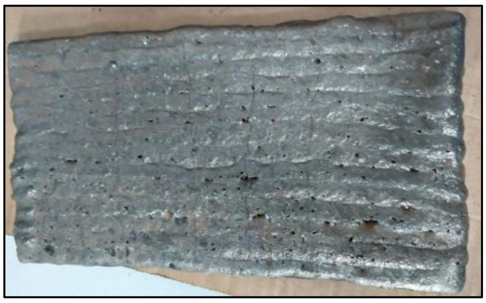

Figure 1. Coated sheet

After the welding procedure, the specimens were subjected to the milling, finishing, and cutting process to proceed with the proposed tests.

## 2.1 Chemical analysis

For the certification of the tested materials, the chemical compositions of the base material and the coated base material were obtained through chemical analysis by spectrometry - iron base carried out at the Material Testing and Analysis Laboratory - LAMAT with the SPECTROMAXx optical emission spectrometer equipment, with samples removed from the base plate and coated plate.

## 2.2 Tensile test

To verify the mechanical properties of the base material and the coated base material, 3 tensile tests (ASTM E8/E8M-11) were performed for each, to determine the stress x strain curves. The tests were carried out with the CIT Senai universal test machine with a maximum load of 1000 kN and the results were obtained through the arithmetic mean of all the values found by the equipment software.

To prepare the stress x strain graph, Eq. 1, and the strain will be calculated with Eq. 2. Elongation and strain were obtained from the arithmetic mean of the data indicated in the test report.

$$\sigma = \frac{F}{A_0}, \tag{1}$$

where σ= engineering stress [MPa], F= applied force [N] and $A_0$= cross-sectional area of the body (before application of load) [ $mm^2$].

$$\varepsilon = \frac{l - l_0}{l_0} = \frac{\Delta l}{l_0}, \tag{2}$$

where ε= engineering deformation, $l_0$= initial length [mm] and l= final length [mm].

The specimens for the test were made by ASTM E8/E8M-11 – Standard Test Methods for Tension Test of Metallic Materials, prepared by the wire EDM machining process with dimensions as shown in Figure 2.

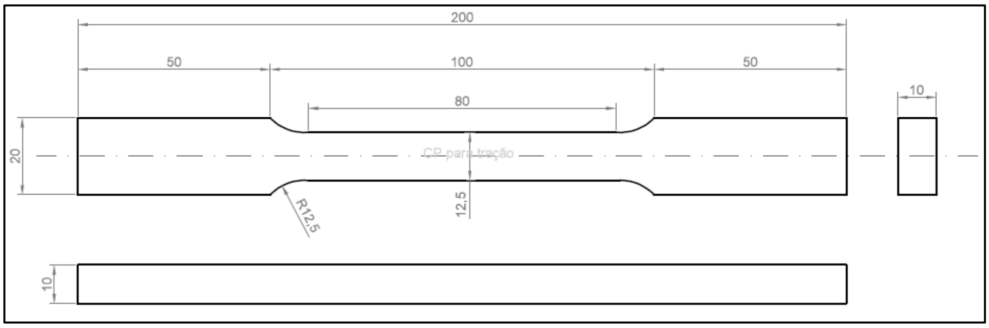


Figure 2. Dimensions of the tensile test specimen

## 2.3 Wear test

To verify wear resistance, pin-on-disk abrasive wear tests were performed following ASTM G99-04. A Microtest tribometer, specifically model SMT-A/0100, serial number B01100-19, of the pin-on-disk type, was used to determine the coefficient of friction (μ) of the specimens with and without coating. Data were collected using the Nanovea Tribometer Software program. The test was carried out without lubrication, at a temperature of 20ºC ± 1ºC. The wear on the base material and the coated base material was measured with the repetition of 3 tests for each situation with the parameters in Table 4.

Table 4. Wear test parameters.

| **Test** | **Pin-on-disk** |
|---|---|
| Speed | 240 rpm |
| Load | 20N |
| Distance | 52 m |
| Track diameter | 5mm |
| Tima | 14 minutes |

The spherical top pins with a diameter of 6 mm used in the test were manufactured with the metal-ceramic composite WC-Co with ultrafine grains in the range of 0.2 to 0.5 µm. The choice of this material is due to the fact that hard materials are materials resistant to wear, due to their hardness and tenacity.

The pin on disk test results in wear on both the pin and the specimen (S) with the formation of wear tracks. After the test, the regions of the worn tracks were subjected to measurement and analysis by profilometry using the HommelwerkT8000 profilometer equipment and the Hommelmap Expert 6 analysis software, to determine the volume of material removed in the S's, the width of the track is obtained through this measurement and analysis. This procedure was performed in three different regions to obtain a reliable average of the results. According to the ASTM-G99 standard, when only the disc shows significant wear, it is possible to determine the volumetric loss of the sample by Eq. 3.

$$Q = \frac{\pi * r_t * (b_t)^3}{6 * r_p}, \tag{3}$$

where $Q$= S volumetric loss [ $mm^3$], $r_t$= radius of the wear track [mm], $b_t$= width of the wear track [mm] and $r_p$= radius of the spherical top of the pin.

The disc wear rate, known as the k coefficient, was calculated according to Archard 's Law, as shown in Eq. 4 depending on the volume lost, the load applied, and the distance covered.

$$k = \frac{Q}{W * D}, \tag{4}$$

where k= wear coefficient [ $\frac{mm^3}{m * N}$], $Q$= S volumetric loss [ $mm^3$], W= normal test load [N] D= distance traveled [m].

The comparison between wear rates in different materials was possible by analyzing the value of the k coefficient. (HUTCHINGS and SHIPWAY, 2017).

# 3. RESULTS

## 3.1 Chemical analysis

The concentrations of the chemical elements present in the base metal in percentage by weight are shown in Table 5. Comparing the results obtained with the manufacturer's analysis in Table 2, it can be observed that the concentration of all the chemical elements present in the base metal is between the stipulated limits.

Table 5 - Chemical composition of Hardox® 450

| C | Si | Mn | P | S | Cr | Ni | Mo | B |
|---|---|---|---|---|---|---|---|---|
| 0.154 | 0.256 | 1,246 | 0.018 | 0.003 | 0.079 | <0.0225 | <0.0045 | 0.0012 |

In the weld metal, the concentrations of chemical elements present in percentage by weight are shown in Table 6, the results are in line with the data presented by the manufacturer in Table 2.

Table 6 - Chemical composition of the welded metal

| C | Si | Mn | P | S | Cr |
|---|---|---|---|---|---|
| 3,617 | 0.862 | 0.912 | 0.010 | 0.008 | 19.28 |

## 3.2 Tensile test

The stress versus strain graph obtained showed very close curves, evidencing uniformity of the mechanical properties of the material in its section, with the average resistance limit of 1,456.11 MPa with a standard deviation of 2.76 Mpa, the average yield stress at 1,326, 72 MPa with a standard deviation of 13.39 Mpa, the average elongation of 16.30% with a standard deviation of 0.75% and the average necking of 57.37% with a standard deviation of 1.88%, below Table 7 with the data described above.

Table 7 - Hardox® 450 tensile test data

| | S1 | S2 | S3 | Average | DP |
|---|---|---|---|---|---|
| Tensile strength (MPa) | 1,453.70 | 1,459.11 | 1,455.51 | 1,456.11 | 2.76 |
| Yield strength (MPa) | 1,339.02 | 1,328.69 | 1,312.47 | 1,326.72 | 13.39 |
| Elongation (%) | 15.60 | 16.20 | 17.10 | 16.30 | 0.75 |
| Yield point (%) | 58.50 | 58.40 | 55.20 | 57.37 | 1.88 |

Next, Figure 3 presents the plotted stress versus strain data.

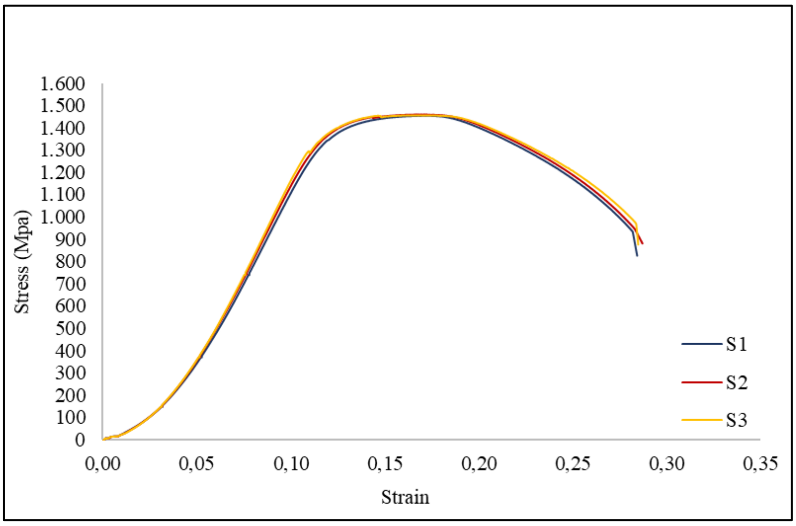


Figure 3. Stress x Strain of Hardox® 450

The stress versus deformation graph of the joints showed different curves, evidencing a non-uniform behavior of the mechanical properties of the welded material. According to the plotted graph and analysis of Table 8, the deposition of the hardfacing through the welding process influenced the mechanical resistance of the coated Hardox® 450.

Table 8 - Tensile test data for coated Hardox® 450

| | S1 | S2 | S3 | Average | DP |
|---|---|---|---|---|---|
| Tensile strength (MPa) | 207.00 | 127.00 | 98.00 | 144.00 | 56.45 |
| Yield strength (MPa) | 189.00 | 121.00 | 93.00 | 134.33 | 49.37 |
| Elongation (%) | 5.40 | 0.20 | 2.00 | 2.53 | 2.64 |
| Yield point (%) | 10.80 | 9.70 | 4.80 | 8.43 | 3.19 |

Next, Figure 4 presents the plotted stress versus strain data.

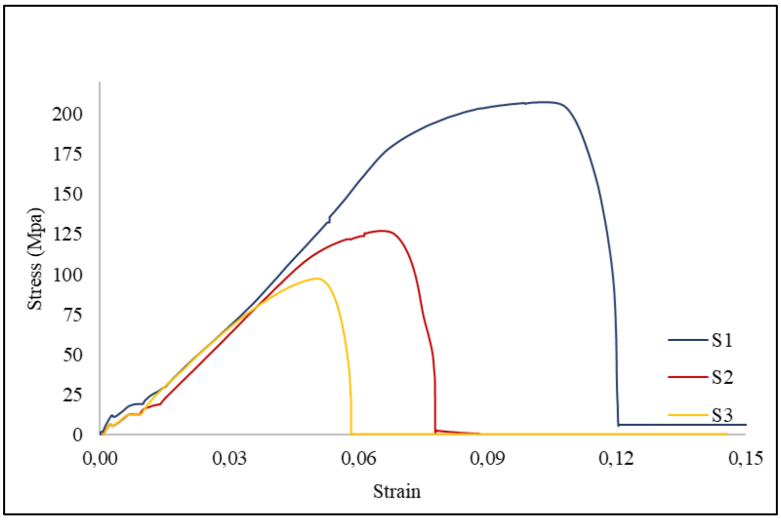


Figure 4. Stress x Strain of coated Hardox® 450

### 3.3 Wear test

The evaluation of wear in the tests was carried out by analyzing the amount of material lost by the specimen about the distance covered during the pin-on-disk test. Figure 5 presents the results of the profilometry of the wear tracks of Hardox® 450 with and without coating, where it was possible to measure the width of the wear tracks based on the red region and obtain the average to use these values in Eq. 3.

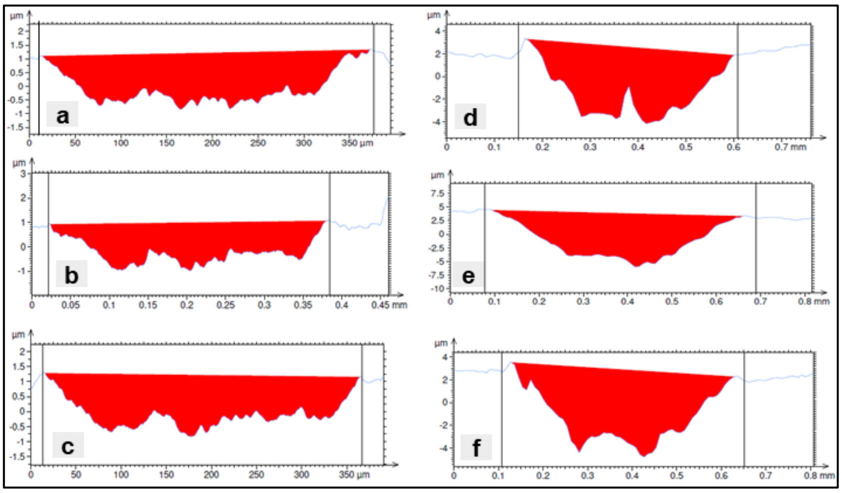


Figure 5. Profilometry of Hardox® 450 wear tracks a, b and c) coated d, e and f) uncoated.

Table 9 shows the volumetric loss values and the wear rate calculated with Eq. 3 and 4 for the coating and Hardox® 450. It is possible to verify that the lost volume and the wear rate were lower for the coating.

Table 9 - Volumetric loss and wear rate values

| | **Hardox® 450 uncoated** | **Hardox® 450 with coating** |
|---|---|---|
| W (N) | 20 | 20 |
| Distance (m) | 52.0 | 51.8 |
| Track width (mm) | 0.5367±0.06 | 0.3583±0.01 |
| Q ( $mm^3$) | 0.6306 | 0.1841 |
| k ( $mm^3/m * N$) | $6.06*10^{-4}$ | $1.77*10^{-4}$ |

The Figure 6 represents the evolution of the coefficient of friction curves (μ) up to 14 minutes. Mean μ values were collected when the curves reached the stationary stage. It was found that the behavior of the μ curves for uncoated Hardox® 450 was similar, however due to the difference in the behavior of the μ curve between S1 and S2 conditions, the third test was necessary. Regarding the μ curves for Hardox® 450 coated with S's 4, 5 and 6, it was observed very close curves with more stability compared to the S1, S2 and S3 curves. This suggests that the steady state was reached after 5 minutes and the μ values remained relatively constant.

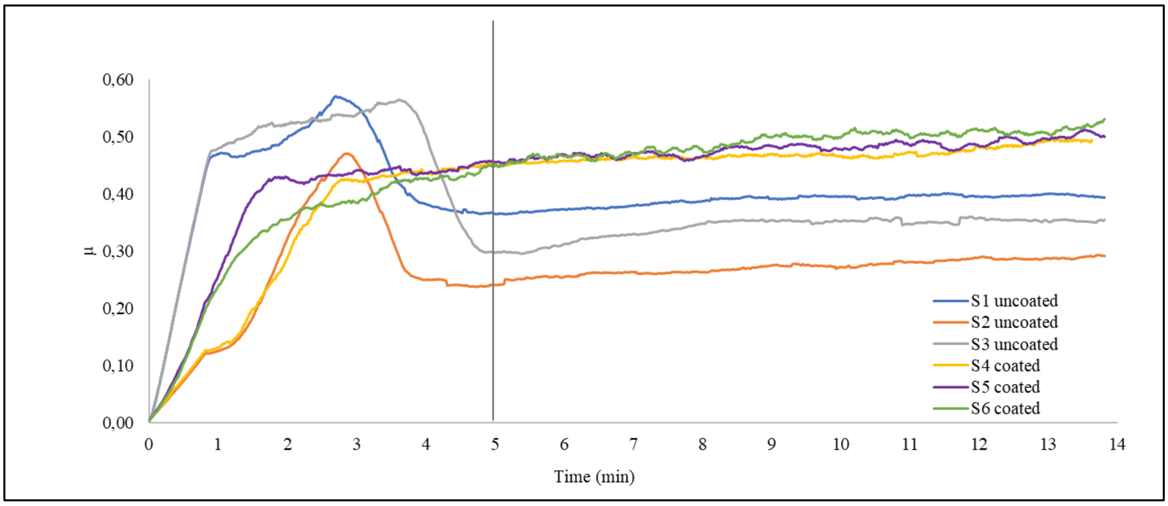


Figure 6. Coefficient of friction during the test period.

The observed variations can be attributed to the presence of debris, which cause instability in the coefficient of friction curve due to deformation and breakage of asperities, this occurs because during the initial phase (run-in), the surfaces in contact are settling. After this, debris is removed from the surface and a real contact area is formed, resulting in friction stabilization (Ba et al., 2021). Table 10 presents μ values for neat and coated Hardox® 450 from the stationary stage.

Table 10 - μ values, volumetric loss and wear rate

| **Hardox® 450** | **Coefficient of friction (μ)** | **Volumetric loss (Q) [ $mm^3$]** | **Wear rate (k) [$10^{-4}$ $mm^3$]/m*N]** |
|---|---|---|---|
| Uncoated (S's 1, 2 and 3) | 0.33 ± 0.05 | 0.6306 | 6.06 |
| Coated (S's 4, 5 and 6) | 0.48 ± 0.01 | 0.1841 | 1.77 |

It is observed that the lowest value of μ was obtained for the uncoated condition. Regarding the coefficient k, the value of the coating was much lower.

## 4. CONCLUSION

When comparing the properties of Hardox 450 and the applied coating, we have the following results:

Comparing the tensile strengths obtained with the test, we can observe that the coated material presented values below those provided by the manufacturers of Hardox® 450 and the coating, these values may be associated with the fact that the tensile strength of the welded metal is 58% lower than the Hardox® 450 and by the welding procedure.

The data obtained from pin-on-disk sliding wear tests indicate that the lowest coefficient of friction was attributed to the base material. Regarding abrasive wear resistance, the coated specimen had a lower volumetric loss (Q) and presented the lowest wear coefficient value (k), these differences may be related to the higher hardness of the coating.

The results indicate that the coating DIN 8555: MF 10-GF-60-GRZ can be considered a good material to be applied in the repairs of the scales, in the recovery of the areas with the highest incidence of wear, thus prolonging the useful life of the equipment.

## 5. ACKNOWLEDGEMENTS

This optional section must be positioned before the list of references.

## 6. REFERENCES

American Society Of Mechanical Engineers. ASME IX BPVC IX: Welding, Brazing and Fusing Qualifications. ASME, 2019

American Society For Testing And Materials. E8/E8M – 11: Standard Test Methods for Tension Testing of Metallic Materials. Conshohocken : ASTM, 2013.

American Society For Testing And Materials. G99-04: Standard Test Method for Wear Testing with a Pin-on-Disk Apparatus. ASTM, 2017.

BA, ECTE; Dumont, MR; Martins, PS; Drummond, RM; Cruz, MPM; Vieira, VF (2021). Investigation of the effects of skewness Rsk and kurtosis Rku on tribological behavior in a pin-on-disk test of surfaces machined by conventional milling and turning processes. Materials Research, 24(2), 1-15.

Costa, AF; Vendramini, JR; Ribeiro, VM Wear analysis of coatings by welding to recover guides of the matrix box feeder made of sae 1045 steel. Vincci Magazine - UniSATC Scientific Journal , [S. l.], v. 4, no. 2, p. 149–178, 2019.

IBRAM. Infographic Mining in numbers. 2021. Available at:< https://ibram.org.br/>. Accessed on: 29 July 2022.

Ivanov, O., et al, Researching of the structure and properties of FCAW hardfacing based on Fe-Ti-Mo-BC welded under low current , Procedia Structural Integrity, v 36, p. 223-230, 2022.

Hutchings, I.; Shipway , P.. Tribology : Friction and Wear of Engineering Materials. 2 ed. Elsevier. 2017

Ligier, K., et al. Analysis of Wear Properties of Hardox Steels in Different Soil Conditions. Materials, 15, 7622, 2022.

OLIVEIRA, Otávio J. Quality management: advanced topics. Cengage Learning, 2020

Özturan , A., et al. Study of the microstructure and mechanical property relationships of gas metal arc welded dissimilar Hardox 450 and S355J2C+N steel joints, Materials Science and Engineering: A, v. 856, 2022.

SSAB. Data sheet 168uk Hardox 450. 2021. Available from: <http://www.ssab.com>. Accessed on: 1 Dec. 2022.

## 7. RESPONSIBILITY NOTICE